PHYSICAL REVIEW E, VOLUME 63, 020601(R)

Crystalline smectic-*B* films as fluctuating systems: Static and dynamic x-ray scattering

Andrea Fera,[1] Igor P. Dolbnya,[2] Ricarda Opitz,[1] Boris I. Ostrovskii,[1,3] and Wim H. de Jeu[1,*]
[1]*FOM-Institute for Atomic and Molecular Physics, Kruislaan 407, 1098 SJ Amsterdam, The Netherlands*
[2]*DUBBLE CRG, ESRF, BP 220, 38043 Grenoble Cedex, France*
[3]*Institute of Crystallography, Academy of Sciences of Russia, Leninsky prospekt 59, 117333 Moscow, Russia*
(Received 2 October 2000; published 11 January 2001)

Static and dynamic x-ray scattering has been used to characterize thermal fluctuations in free-standing smectic films in the crystalline-*B* phase. The results are remarkably similar to those in smectic-*A* films, in spite of the three-dimensional positional order in the crystalline-*B* phase. The main difference is the disappearance of the characteristic Landau-Peierls instability of the smectic-*A* phase. The dynamic nature of the fluctuations is explicitly demonstrated by x-ray photon correlation spectroscopy. This fluctuation behavior of crystalline-*B* films can be attributed to the small value of the shear elastic constant C_{44}.

DOI: 10.1103/PhysRevE.63.020601 PACS number(s): 61.30.−v, 61.10.Kw, 62.20.Dc, 42.25.Kb

Large-scale thermal fluctuations are one of the striking features of systems with reduced translational order. While three-dimensional (3D) crystals exhibit true long-range positional order, such positional order is destroyed by thermal fluctuations in two-dimensional (2D) and one-dimensional (1D) systems [1]. However, similar effects may be observed in a real 3D medium. A classical example is the Landau-Peierls instability in smectic-*A* (Sm-*A*) liquid crystals. A Sm-*A* phase consists of a stack of fluid layers, in which rodlike molecules form a density wave in the direction along the layer normal while the system remains fluid in the other two. In such systems the mean-squared layer displacements $\langle u^2(\mathbf{r})\rangle$ diverge logarithmically with the sample size. In addition to the Sm-*A* phase, a crystalline *B* (Cr-*B*) phase with a hexagonal in-plane lattice may be found at lower temperatures [2]. The exact nature of the Cr-*B* phase has been an intriguing question for quite some time [3]. In the late 1970s the 3D nature of the long-range positional order had been established by x-ray diffraction [4,5]. These results were confirmed by the observation of a solidlike shear response (with elastic constant C_{44}) between the Cr-*B* layers [6]. As a consequence, a term proportional to $C_{44}q^2$ occurs in the elastic free energy, which eliminates the Landau-Peierls instability. Nevertheless, intense diffuse scattering in the vicinity of the Bragg peaks has been observed [4], tentatively interpreted as due to soft shear waves. Indeed, the corresponding shear modulus was found to be about several orders of magnitude smaller than the other elastic constants [7]. In this Rapid Communication we give conclusive experimental evidence that the Cr-*B* phase is a strongly fluctuating system. From x-ray reflectivity of freely suspended smectic films, the spectral dependence of the fluctuations in the Cr-*B* phase is found to be very similar to that in the Sm-*A* phase. However, from the fluctuation profiles for various film thickness, the absence of the Landau-Peierls divergence can be explicitly contrasted with the Sm-*A* situation. The dynamic nature of the fluctuations is demonstrated by x-ray photon correlation spectroscopy, thus excluding any other interpretation of the static x-ray observations.

The compound investigated, *N*-(4-*n*-butoxybenzilidene)-4-*n*-octylaniline, abbreviated as 4O.8, was obtained from Frinton Laboratories, Inc., and used as received. It undergoes the following phase transformations (in °C): K 33 Cr-*B* 48.5 Sm-*A* 63.5 N 78 I. Freely suspended smectic films were spanned over a $10\times 23\,\mathrm{mm}^2$ hole in a stainless steel frame and equilibrated as described earlier [8]. Such films have a high degree of uniformity and a controlled thickness ranging from two to over hundreds of layers. They were mounted in a temperature controlled two-stage oven and evacuated to $<10^3$ Pa in order to prevent possible sample degradation and reduce air scattering.

X-ray reflectivity measurements were carried out at beamline BW2 of HASYLAB (DESY, Hamburg) at an energy of 10.0 keV. We used three types of scans to characterize our films as shown in Fig. 1, where also the wave-vector transfer $\mathbf{q}=\mathbf{k}_f-\mathbf{k}_i$ is defined. Specular scans probe the scattered intensity in the reciprocal space along q_z with $q_x=q_y=0$. The quality of the sample was monitored by measuring rocking curves at different q_z, varying q_x by rotation of the sample. The mosaicity of a Sm-*A* film was typically 0.002° full width at half maximum (FWHM). Transverse diffuse scans probe the scattered intensity along q_y at fixed q_z by moving the detector out of the plane of specular reflection. The scans were made across the first Bragg sheet corresponding to $q_z=2\pi/d=2.21\,\mathrm{nm}^{-1}$, where d is the smectic layer periodicity. Note that correlations probed in q_y are equivalent to those in q_x as the Sm-*A* samples are liquid in the *xy*-plane (indicated as $q_\perp$). The same equivalence holds for the Cr-*B*

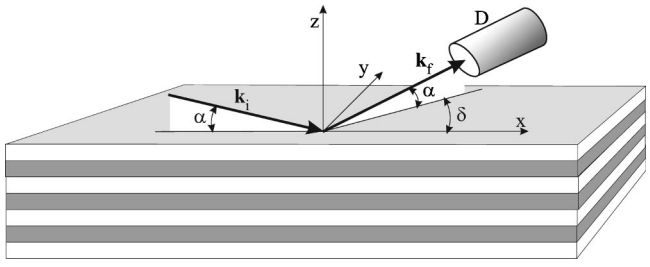

FIG. 1. Scattering geometry. In transverse diffuse scans q_y is varied at fixed q_z (determined by $\alpha=\beta$) by moving the detector out of the scattering plane.

*Corresponding author. Email address: dejeu@amolf.nl

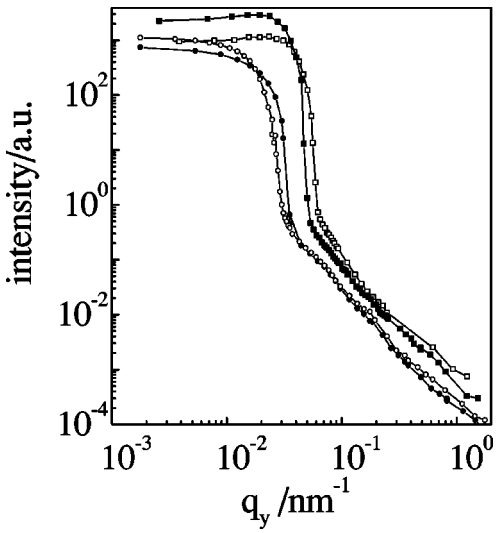

FIG. 2. Transverse diffuse scans for an eight layer (circles) and an 80 layer (squares) film at the first Bragg peak. Closed symbols Sm-*A* phase; open symbols, Cr-*B* phase. The solid lines are given as a guide to the eye.

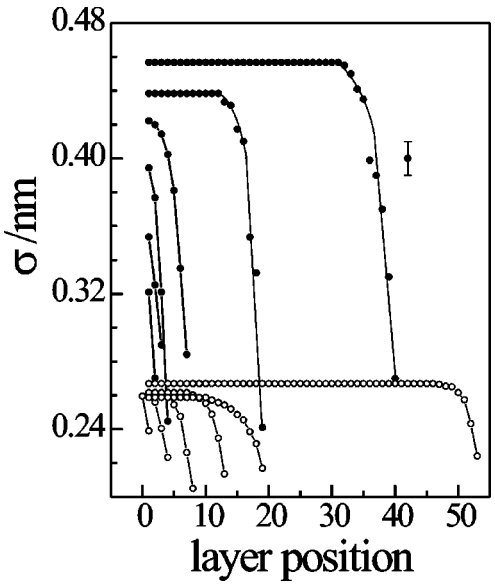

FIG. 3. Fluctuation profiles in the Sm-*A* phase (around 63 °C, closed circles, 5, 6, 8, 15, 38, and 80 layers) and in the Cr-*B* phase (around 47 °C, open circles, 3, 8, 16, 26, 38, and 107 layers) as derived from modeling the specular reflectivity data as described in the text. A resulting error bar is indicated.

phase due to the mosaic averaging of the hexagonal in-plane lattice. The experimental resolution [9] was set by slits to $\Delta q_x \approx 4\times10^{-3}\,\mathrm{nm}^{-1}$, $\Delta q_y \approx 0.02\,\mathrm{nm}^{-1}$, and $\Delta q_z \approx 0.04\,\mathrm{nm}^{-1}$. For the thickest films, these values were changed to $\Delta q_x \approx 2\times10^{-3}\,\mathrm{nm}^{-1}$, $\Delta q_y \approx 0.05\,\mathrm{nm}^{-1}$, and $\Delta q_z \approx 0.01\,\mathrm{nm}^{-1}$. This allowed us to determine in all curves the number of layers in each film from the reflectivity oscillations (Kiessig fringes). X-ray photon correlation spectroscopy was performed at the undulator beamline ID10A (Troika I) at the European Synchrotron Radiation Facility (ESRF, Grenoble) with 7.98-keV radiation. Details of the procedure have been given elsewhere [10,11]. In short, a circular pinhole of 12 μm was placed at 45 m from the source and 0.25 m upstream of the sample in order to provide a collimated and partially coherent beam. The intensity-intensity time correlation function $G^{(2)}(\mathbf{q},t) = \langle I(\mathbf{q},0)I(\mathbf{q},t)\rangle$ was recorded at the first Bragg peak with a resolution given by $\Delta q_z = \Delta q_y \approx 10^{-3}\,\mathrm{nm}^{-1}$ and $\Delta q_x \approx 10^{-4}\,\mathrm{nm}^{-1}$.

Transverse diffuse scans for 8 and 80 layer films are shown in Fig. 2. For both films, only small changes are seen between the results for the Sm-*A* and the Cr-*B* phase. Specular and diffuse x-ray scattering from freely suspended Sm-*A* films has been well studied both experimentally [8] and theoretically [12]. The reflected intensity $I(\mathbf{q})$ can be written within the first Born approximation as the Fourier transform of the interlayer displacement-displacement correlation function $G(\mathbf{r}) = G(\mathbf{r}_\perp, z, z') = \langle u(\mathbf{r}_\perp, z)u(0,z')\rangle$ convolved with an experimental resolution [8]. $G(\mathbf{r}_\perp, z, z')$ depends on the surface tension γ and the elastic constants for compression (B) and bending (K) of the smectic layers. Explicit expressions for $G(\mathbf{r}_\perp, z, z')$ and $I(\mathbf{q})$ have been given in Ref. [8]. A full discussion of the fitting procedure will be given elsewhere. For the present purpose, we note that the difference between the Sm-*A* and Cr-*B* results can be accounted for by an increase of the effective surface tension γ_{eff} from 0.02 to about 0.03 N/m. Hence the fluctuations in Cr-*B* films can be described essentially by the same hydrodynamic model as used for Sm-*A* films.

To test the above results further, specular scans taken in the Sm-*A* and Cr-*B* phases were compared. The specular data were fitted with an iterative matrix solution of the Fresnel equations for the reflectivity of the multilayer system using a slab-model for the electron density profiles. Each smectic layer was approximated by a boxlike function, convoluted with a Gaussian of width σ_i to take the fluctuations of the layers into account [8]. The resulting centrosymmetric σ_i profiles are depicted in Fig. 3 for one half of Sm-*A* and Cr-*B* films of different thickness. The layer fluctuations are quenched at the free surfaces where the σ-values are nearly independent of the number of smectic layers. In the Sm-*A* phase, the amplitude of the fluctuations in the middle increases as a function of the film thickness, which is a direct signature of the Landau-Peierls instability [13]. In contrast, in the Cr-*B* phase, the amplitude of the fluctuations in the interior of the film does not depend on the film thickness. Nevertheless, the fluctuations in the center remain relatively large, about 0.25 nm. Moreover, the fluctuations of the surface layers are quenched similarly as in the Sm-*A* phase. The total picture indicates (nondiverging) thermal layer fluctuations in the Cr-*B* phase.

The dynamic nature of the fluctuations in Cr-*B* films is explicitly demonstrated by a measurement of the of the intensity-intensity autocorrelation function $G^{(2)}(\mathbf{q},t)$, see Fig. 4. The behavior of the correlation function is very similar to that reported earlier for Sm-*A* films [11]. It can be described by an exponential decay of which the amplitude is modulated by a cosine function. The associated relaxation time is $\tau = 4.9 \pm 0.5\,\mu$s, while the oscillatory behavior has a

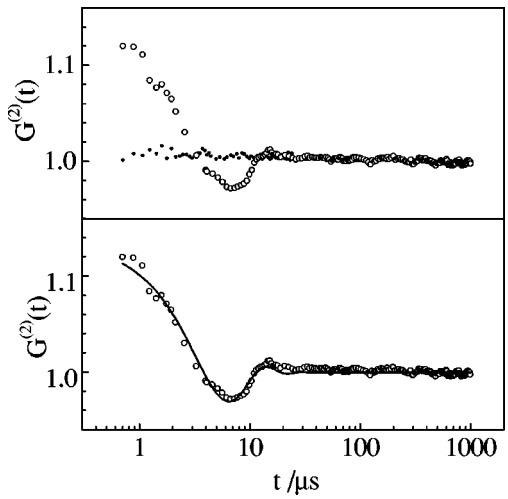

FIG. 4. Intensity-intensity autocorrelation function of a 0.27-μm film in the Cr-*B* phase ($T=46\,^{\circ}$C). (a) Raw data (open dots) and reference signal from the NiC multilayer (closed dots). (b) Normalized correlation function.

period given by $2\pi/\omega=15.1\pm0.3\,\mu$s. In fact, these times hardly change upon heating into the Sm-*A* phase.

To describe the elasticity of the Cr-*B* phase, the standard elastic theory of a hexagonal crystal can be applied. However, in the present situation the shear constant C_{44} is much smaller than the other ones: $C_{44}/C_{11}\approx10^{-5}$ [6,7]. Hence, we can apply the approximation that, apart from shear, all deformations are forbidden. In this easy-shear approximation, the elastic free energy of a freely suspended Cr-*B* film may be written as [13]

$$F=\tfrac{1}{2}\int d^3\mathbf{r}\left[B\left(\frac{\partial u(\mathbf{r})}{\partial z}\right)^2+K[\Delta_\perp u(\mathbf{r})]^2+\tfrac{1}{2}C_{44}[\nabla_\perp u(\mathbf{r})]^2\right]$$
$$+\tfrac{1}{2}\gamma\int d^2\mathbf{r}[\nabla_\perp u(\mathbf{r}_\perp,z=\pm\tfrac{1}{2}L)]^2.$$

The boundaries of the film are at $z=\pm L/2$, where $L=Nd$ is the thickness of an N-layer film. The presence of the term with C_{44} (which gives the difference compared to a Sm-*A* film and removes the Landau-Peierls instability) does not affect the layer compression and bending rigidity. The main effect of incorporating the Cr-*B* lattice via C_{44} can be seen as an effective renormalization of the surface tension: $\gamma_{\rm eff}\approx\gamma+LC_{44}/4$. Using $\gamma=0.02$ N/m [15] and $C_{44}=0.12\times10^6\,\mathrm{N/m^2}$ [6], we calculate that the correction only becomes appreciable for rather thick films and is equal to γ for about 230 layers. However, γ itself might also increase upon going from Sm-*A* to Cr-*B* [16]. The observed increase in $\gamma_{\rm eff}$ does not allow one to discriminate between these two possible contributions. Nevertheless, these considerations indicate that Cr-*B* films can be considered as fluctuating systems rather similar to Sm-*A* films, in agreement with our experiments.

Finally we want to comment on the dynamic measurements. Investigation of the dynamic properties of the Sm-*A* Hamiltonian [14,17,18] involves a demanding calculation of the time-dependent correlation function $G(\mathbf{q}_\perp,z,z',t)=\langle u(\mathbf{q}_\perp,z,0)u^*(\mathbf{q}_\perp,z',t)\rangle$. In the simplest approximation, this can be done by equating the viscous and elastic forces, while neglecting inertia. Further assuming incompressible films and conformal fluctuations, for Sm-*A* films, a spectrum of relaxation modes is found which for $q_\perp=0$ reduces to a single fundamental relaxation time $\tau=\eta_3 L(2\gamma)$. Here η_3 is the viscosity associated with shear of the layers. This equation can, in a first approximation, be extended to the Cr-*B* phase by again replacing γ by $\gamma_{\rm eff}$. Reference [14] gives a more complete discussion of the dynamics of Cr-*B* films. For the present purpose, within the above approximations, the fundamental relaxation time is not expected to change much on going from Sm-*A* to Cr-*B* in a not very thick film, in agreement with the experiments. As has been shown elsewhere for Sm-*A* films [11], the situation is more complicated in the thin film regime than has been described so far because inertia cannot be neglected. As a consequence, the relaxation time appears to be complex in the long wavelength limit: the real part corresponds to relaxation, while the imaginary part produces oscillations in the correlation functions. Indeed, the same behavior is observed for Cr-*B* thin films.

In conclusion, we have used static and dynamic x-ray scattering to characterize thermal fluctuations in free-standing smectic films. We find that although the Cr-*B* phase has 3D positional order, thermally driven fluctuations occur in Cr-*B* films that are remarkably similar to those in Sm-*A* films. This is due to the small shear elastic constant C_{44} in the Cr-*B* phase, which allows for the use of an easy shear approximation to the elastic free energy. The dynamic nature of the Cr-*B* fluctuations has been confirmed by x-ray correlation spectroscopy, which shows a complex relaxation behavior in the microsecond range.

We want to thank Arcadi Shalaginov for valuable discussions on the theory and Gerhard Grübel (ESRF) for help with the dynamic x-ray measurements. Work at HASYLAB was supported by the TMR—Contract ERBFMGECT950059 of the European Community. This work was part of the research program of the ''Stichting voor Fundamenteel Onderzoek der Materie, (FOM),'' which is financially supported by the ''Nederlandse Organisatie voor Wetenschappelijk Onderzoek, (NWO).''

[1] See, for example, P. M. Chaikin and T. C. Lubensky, *Principles of Condensed Matter Physics* (Cambridge University Press, Cambridge, England, 1995).

[2] See, for example, G. Vertogen and W. H. de Jeu, *Thermotropic Liquid Crystals, Fundamentals*, Vol. 45 of Chemical Physics (Springer, Berlin, 1988).

[3] See, for example, P. S. Pershan, *Structure of Liquid Crystal Phases* (World Scientific, Singapore, 1988), and references

therein.

[4] D. E. Moncton and R. Pindak, Phys. Rev. Lett. **43**, 701 (1979).

[5] A. J. Leadbetter, J. C. Frost, and M. A. Mazid, J. Phys. (France) Lett. **40**, L-325 (1979).

[6] R. Pindak, D. J. Bishop, and W. O. Sprenger, Phys. Rev. Lett. **44**, 1461 (1980); M. Cagnon and G. Durand, Phys. Rev. Lett. **45**, 1418 (1980).

[7] E. Dubois-Violette, B. Pansu, P. Davidson, and A. M. Levelut, J. Phys. (France) II **3**, 395 (1993), and references therein.

[8] E. A. L. Mol, J. D. Schindler, A. N. Shalaginov, and W. H. de Jeu, Phys. Rev. E **54**, 536 (1996); E. A. L. Mol, G. C. L. Wong, J.-M. Petit, F. Rieutord, and W. H. de Jeu, Phys. Rev. Lett. **79**, 3439 (1997); A. Fera, D. Sentenac, B. I. Ostrovskii, I. Samoilenko, and W. H. de Jeu, Phys. Rev. E **60**, R5033 (1999).

[9] D. Sentenac, A. Shalaginov, A. Fera, and W. H. de Jeu, J. Appl. Crystallogr. **33**, 130 (2000); D. Sentenac, A. Fera, R. Opitz, B. I. Ostrovskii, O. Bunk, and W. H. de Jeu, Physica B **283**, 232 (2000).

[10] G. Grübel and D. Abernathy, SPIE **3154**, 103 (1997); D. L. Abernathy, G. Grübel, S. Brauer, I. Mc Nulty, G. B. Stephenson, S. G. J. Mochrie, A. R. Sandy, N. Mulders, and M. Sutton, J. Synchrotron Radiat. **5**, 37 (1998).

[11] A. Fera, I. P. Dolbnya, G. Grübel, H. G. Muller, B. I. Ostrovskii, A. N. Shalaginov, and W. H. de Jeu, Phys. Rev. Lett. **85**, 2316 (2000).

[12] R. Holyst, Phys. Rev. A **42**, 7511 (1990); **44**, 3692 (1991); A. Shalaginov and V. P. Romanov, Phys. Rev. E **48**, 1073 (1993).

[13] Using typical values for B and K [8] in the Sm-A phase, one can calculate [1,2] the bulk value of σ for an 8 and 80 layer film, resulting in 0.16 and 0.24 nm, respectively. These values are smaller than the observed ones in the middle of the film (Fig. 3). This probably means that the values of B and/or K used must be reconsidered.

[14] A. N. Shalaginov and D. E. Sullivan, Phys. Rev. E **62**, 699 (2000).

[15] P. Mach *et al.*, Langmuir **14**, 4330 (1998).

[16] K. Miyano, Phys. Rev. A **26**, 1820 (1982).

[17] A. C. Price, L. B. Sorensen, S. D. Kevan, J. Toner, A. Poniewerski, and R. Holyst, Phys. Rev. Lett. **82**, 755 (1999); A. Poniewerski, R. Holyst, A. C. Price, L. B. Sorensen, S. D. Kevan, and J. Toner, Phys. Rev. E **58**, 2027 (1998); A. Poniewerski, R. Holyst, A. C. Price, and L. B. Sorensen *ibid.* **59**, 3048 (1999).

[18] H. Y. Chen and D. Jasnow, Phys. Rev. Lett. **61**, 493 (2000).